RESEARCH ARTICLE

Linear (–)-Zampanolide: Flexibility in Conformation-Activity Relationships

Christian A. Umaña[a], Jeffrey L. Henry[a], Claire T. Saltzman[a], Dan L. Sackett[b], Lisa M. Jenkins[c], and Richard E. Taylor*[a]

[a] C. A. Umaña, Dr. J. L. Henry, C. T. Saltzman, Prof. Dr. R. E. Taylor
Department of Chemistry and Biochemistry and the Warren Center for Drug Discovery
University of Notre Dame
Notre Dame, IN 46556-5670, USA
E-mail: rtaylor@nd.edu
[b] Dr. D. L. Sackett
Eunice Kennedy Shriver National Institute of Child Health and Human Development
National Institutes of Health
Bethesda, MD 20892, USA
E-mail: sackettd@mail.nih.gov
[c] Dr. Lisa Jenkins
Center for Cancer Research
National Cancer Institute
Bethesda, MD 20892
E-mail: jenkinsl@mail.nih.gov

Supporting information for this article is given via a link at the end of the document.

Supporting information for this article is given via a link at the end of the document.

Abstract: Through an understanding of the conformational preferences of the polyketide natural product (–)-zampanolide, and the structural motifs that control these preferences, we developed a linear zampanolide analogue that exhibits potent cytotoxicity against cancer cell lines. This discovery provides a set of three structural handles for further structure-activity relationship (SAR) studies of this potent microtubule- stabilizing agent. Moreover, it provides additional evidence of the complex relationship between ligand preorganization, conformational flexibility, and biological potency.

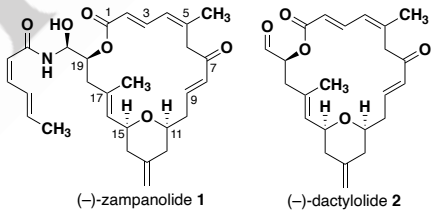

Figure 1. Marine natural products zampanolide and dactylolide.

Introduction

Conformational flexibility is an important feature exhibited in polyketide natural products and impacts their biological and physical properties. Inspired by the seminal contributions of Hoffman, our lab and others have now revealed that these molecules exist in solution as a group of conformational families and that one of these highly-populated conformations resembles the required active-site shape necessary to exhibit potent biological activity.[1] Classical structure-activity relationships (SAR) focus predominantly on improving non-covalent interactions between a ligand and a protein's binding site. This effort often seeks to enhance the enthalpic component of the ligand-protein binding event, often disregarding the impact of the conformational flexibility in the process of analog design particularly for complex structures with multiple rotatable bonds.[1b,2] Understanding the complex relationship between structural modifications and their conformational influence continues to be an under-appreciated component of natural product analogue design.[3]

(–)-Zampanolide **1** (Figure 1) is a natural product isolated in 1996 from the marine sponge *Fasciospongia rimosa*, which possesses a highly unsaturated 20-membered macrolactone, with few stereocenters and an unusually stable *N*-acyl hemiaminal side chain.[4] This microtubule-stabilizing agent exhibits potent antiproliferative activity against numerous cancer lines and has shown superior activity against cell lines with P-glycoprotein overexpression, the principal cancer resistance pathway against multiple drugs like the vinca alkaloids and taxanes.[5] In 2001, (–)-dactylolide **2** (Figure 1) was isolated, a natural product that shares the same macrocyclic core as **1** but lacks the novel *N*-acyl hemiaminal side chain.[6] In 2018, the Northcote group isolated five natural analogues of **1** which displayed nanomolar cytotoxicity towards HeLa cells, except for the C8-C9 saturated analog.[7] The activity of these congeners, along with zampanolide-tubulin covalent interactions observed in the X-ray crystal structure, [8] highlighted the α,β-unsaturated ketone, and the *N*-acyl hemiaminal side chain as two functional "hotspots" essential to potent biological activity.[9] Additionally, Northcote's report provided the first co-isolation of **1** and **2** implying a common or related biosynthetic pathway.[7]

Several years ago, our lab reported a detailed analysis of the solution conformational preferences for these macrocycles. Our combined computational and experimental effort identified three main conformational families in solution including one which was shown to have significant similarity to that observed in a cocrystal structure of **1** bound to an α,β-tubulin subunit.[8,10] We observed the C2-C9 region to be dynamic, while in contrast, the tetrahydropyran and the 16,17-trisubstituted alkene exhibited much less conformational flexibility. The latter was rigidified, in part, by minimization of the $A^{1,3}$-strain generated from the steric repulsion between the C17-methyl and the C15 allylic stereocenter. We recently confirmed the significance of this conformational control element through the preparation of a C17-desmethyl analogs of dactylolide and zampanolide. Removal of the C17-methyl enables greater torsional flexibility on both sides of the 16,17-olefin at the expense of potent biological activity.[11] This result is in agreement with the loss of biological potency observed by the Altmann group in their synthesis of des-tetrahydropyran[12] and pyrazole[13] analogs.

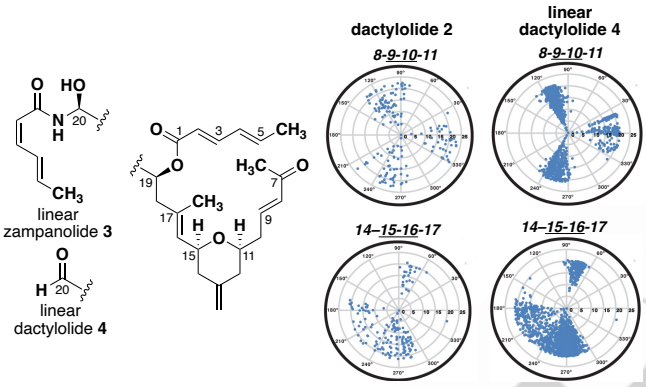

Figure 2. Proposed linear analogs **3** and **4**. Selected dihedral angle distribution plots for dactylolide and the acyclic variant **4** from computational modeling. A complete description of the polar plots can be found on the SI.

Results and Discussion

Based on the emerging conformation-activity relationship profile for these natural products,[7,8,11] we hypothesized that linear analog **3** (Figure 2) would retain potent biological activity, with torsional constraints provided by the southern region remaining intact. We first conducted a comparative conformational search using a 50,000-step Monte Carlo search employing the MM3* force field [14] in conjunction with the GB/SA solvation model for water (Figure 2). Structures within 4.7 kcal/mol of the global minimum were saved and the duplicated conformers were eliminated to yield a potential energy surface of conformational families. [15] To simplify the computational study, the C19-aldehyde (dactylolide congener) was used in both the macrocyclic and linear starting structures.[10] Analysis of the polar coordinate maps for torsions with **3** and **4** suggested that while higher degree of torsional flexibility and a flatter potential energy surface is observed in the linear structure, highly-populated conformational families were similar to the parent macrolide. It is important to note that the conformational preferences on the C15-C18 section show few differences compared to **2**, suggesting that the $A^{1,3}$-strain about the C15-C16 dihedral still dictates the conformational preferences of the linear analogue. As was recently demonstrated by Karlén and coworkers, linear structures are just as likely to populate biologically active conformations given proper inclusion of other conformational control elements.[16]

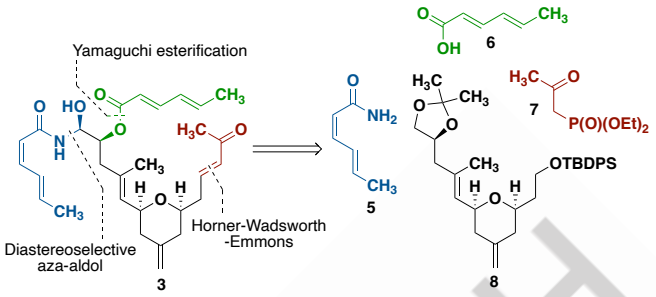

Scheme 1. Retrosynthetic analysis for acyclic zampanolide **3**.

The retrosynthetic analysis presented on Scheme 1, highlights use of Altman's diastereoselective aza-aldol with diene-amide **5** for the installation of the *N*-acyl hemiaminal side chain,[17] a Yamaguchi esterification with sorbic acid **6** to install the C19 acyl group, and a Horner-Wadsworth-Emmons (HWE) olefination with diethyl (2-oxopropyl)phosphonate **7** to prepare the α,β-unsaturated ketone. Our strategy recognized the complex tetrahydropyran **8** as a key linchpin for this triply-convergent strategy. Access to **8** could be achieved through the synthetic sequence previously developed in our lab for the synthesis of **1** and highlighted by our ether-transfer methodology.[18,19]

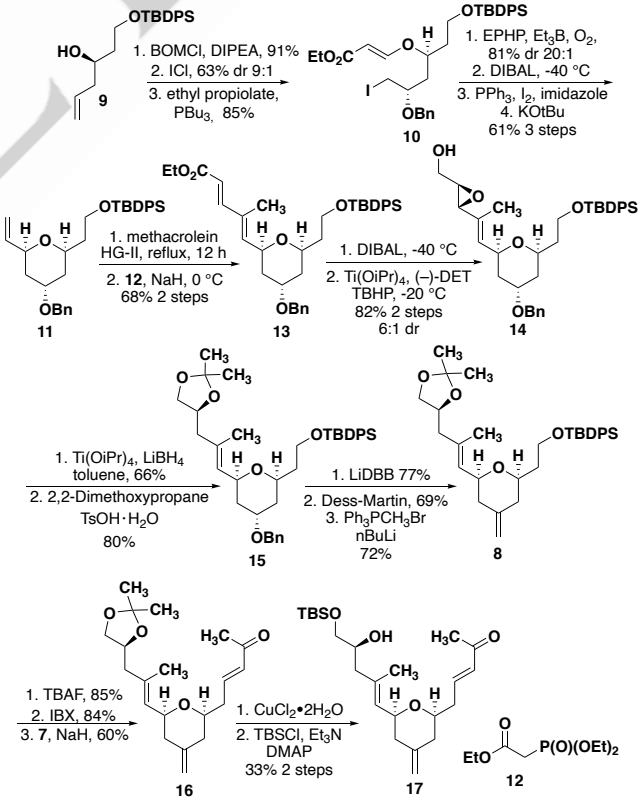

Scheme 2. Synthesis of α,β-unsaturated ketone **17**.

Our synthesis started from the enantiomerically pure alcohol **9** prepared from (*R*)-aspartic acid over three steps.[12] Alcohol **9** was alkylated with benzyloxy methyl ether to yield the BOM ether, followed by diastereoselective electrophilic activation with ICl,[19] and conjugate addition to ethyl propiolate promoted with tributyl phosphine to give the β-alcoxyacrylate **10** in good yield. An intramolecular radical cyclization catalyzed by triethylborane in the presence of 1-ethylpiperidinium hypophosphate (EPHP) gave excellent yield and diastereoselectivity, followed by an ester reduction with DIBAL, iodination of the primary alcohol and subsequent elimination under basic conditions delivered the terminal olefin **11**. Preparation of the conjugate dienonate **13** was achieved by a cross-metathesis with methacrolein in the presence of Hoveyda-Grubbs II catalyst (HG-II), followed by HWE olefination with triethyl phosphonoacetate **12**. Ethyl ester **13** reduction and diastereoselective Sharpless epoxidation provided epoxy-alcohol **14** in good yields and generated the C19-stereogenic center. Hydride epoxide opening catalyzed by $Ti(OiPr)_4$ and acetalization with 2,2-dimethoxypropane under acidic conditions furnished acetonide **15**. To install the exo-methylene on the tetrahydropyran ring, a three-step sequence involving reductive benzyl deprotection with 4,4'-di-tert-butylbiphenylide (LiDBB), oxidation with Dess-Martin periodinane and Wittig olefination with methyltriphenyl phosphonium bromide, delivered good yields to obtain **8**. The eastern derivatization started with silyl deprotection promoted by TBAF, followed by alcohol oxidation with IBX that provided a milder environment for the acidic labile acetonide, in comparison with the commonly used Dess-Martin periodinane. HWE olefination with **7** delivered exclusively *E*-isomer for the α,β-unsaturated ketone **16** in good yield. Acetonide hydrolysis mediated by $CuCl_2$ and subsequent regioselective TBS protection of the primary alcohol afforded alcohol **17** in low yields.

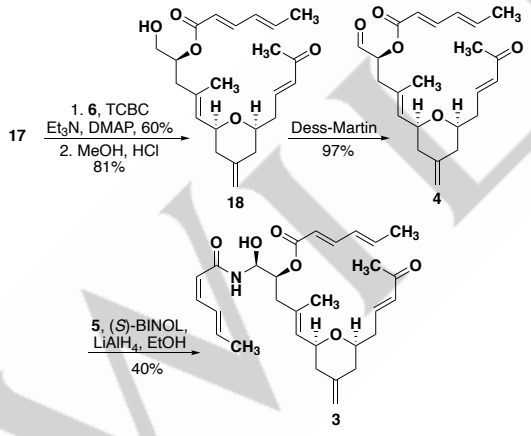

Scheme 3. Completion of linear dactylolide **4** and zampanolide **3**.

The end game towards **3** (Scheme 3) started with a Yamaguchi esterification with **6** and silyl ether deprotection under acidic methanol to yield alcohol **18**. Dess-Martin oxidation provided linear dactylolide **4** in excellent yield and, at this point, a diastereoselective aza-aldol, an elegant, recent contribution from the Altmann lab, was utilized for the installation of the hemiaminal side chain.[17] Unfortunately, this transformation resulted in low conversion. However, after chromatographic separation and purification a single diastereomer of linear zampanolide **3** was isolated in 25 steps as the longest linear sequence starting from homoallylic alcohol **9**.

In an effort to confirm the conformational profile predicted by the computational analysis, we performed two-dimensional NMR experiments on **4** and studied the compound's conformational preferences in solution. ROESY experiments were acquired in DMSO on an 800 MHz spectrometer with 500 ms and 800 ms as mixing times, to discriminate between strong and weak correlations, respectively. It was observed from the data acquired that the C2-C5 (zampanolide numbering) diene section presented more flexibility, in a mixture of predominantly *s-trans* over *s-cis* diene, with both protons H4 and H5 displaying spatial-interactions with the H6 protons. Over the C7-C10 section, strong interactions were observed between H12 and H8 and H9, at both mixing times, which suggest no distinguishable preferred conformation for that section. According to the computational predictions, the C7-C10 section exhibits a high degree of rotation, and this was visualized from the ^{1}H-NMR signal averaging of the C10 protons, 7.5 Hz ($^3J_{H10\text{-}H9}$) and 6.1 Hz ($^3J_{H10\text{-}H11}$). Within the C15-C18 section of **4**, C17-methyl presented strong interactions with H15 and H19, and H16 displayed strong interactions with protons at C18 (Conformer 4a, Figure 3). Although, weak interactions were found between C17-methyl and protons at C18, and between H16 and H19 (Conformer 4b, Figure 3), interactions not seen at the parent natural product **2**, as the presence of the macrolide constrains the necessary rotations to allow those interactions. Conformational flexibility in this region was further supported by H18-H19 coupling values ($^3J_{H19\text{-}H18a}$ = 9.0 Hz and $^3J_{H19\text{-}H18b}$ = 4.8 Hz) contrast with the previously reported ($^3J_{H19\text{-}H18a}$ = 11.2 Hz and $^3J_{H19\text{-}H18b}$ = 2.7 Hz).[10]

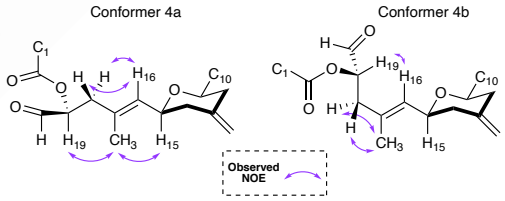

Figure 3. Observed NOEs along the C15-C19 region for two main conformers of linear analog **4**. While conformer 4a mimics the natural series, conformer 4b is only possible by the removal of the constraints provided by the macrocycle.

The spectral data analysis in conjunction with the computational models supported our initial hypothesis, the C2-C5 and C7-C10 sections of linear **4** are allowed to populate a significantly larger conformation ensemble than macrocycle **2** and even, C17-desmethyl analogs previously discussed. However, the rigidity of the C15-C18 section is still controlled by the minimization of $A^{1,3}$-strain about the C15-C16 torsion. In an effort to correlate the increased torsional flexibility of the linear analogs with the biological activity, the growth inhibition (GI_{50}) of the compounds was tested in prostate (PC3), lung (A549), and ovarian (1A9) human carcinoma cell lines and compared with paclitaxel and the parent natural products zampanolide and dactylolide (Table 1).

Table 1. Antiproliferative activity of linear analogs of zampanolide (ZMP) and dactylolide (DAC) on human carcinoma cell lines.

Compound[a] GI_{50} (nM)	PC3	A549	1A9
(-)-zampanolide	0.6 ± 0.2	1.00 ± 0.36	0.6 ± 0.1
(-)-dactylolide	160 ± 10	900 ± 200	150 ± 30
3	40 ± 20	600 ± 360	50 ± 10
4	1400 ± 400	4000 ± 900	2400 ± 1400
18	1900 ± 700	> 6000	3200 ± 1300
paclitaxel	1.3 ± 1.1	0.5 ± 0.2	4.2 ± 0.5

[a] Cells were exposed to the compounds for 72 h.

Linear zampanolide **3** displayed good cytotoxicity against a range of cell lines, although it did not fully replicate the potency of natural zampanolide. Despite populating a larger conformational ensemble than the previously described macrocyclic 17-desmethyl analogs, the linear compound was more active. These results exemplify the critical role that the C16-C17-trisubstituted olefin has in the control of the conformational landscape of zampanolide. This is an effect that is also seen with the *N*-acetyl morpholine-based zampanolide prepared by the Altmann group.[20] Not surprisingly, analogs of dactylolide **4** and **18** did not display significant activity. In contrast to zampanolide, structural modifications of dactylolide have typically resulted in a significant loss of cytotoxicity. This is likely due to structural differences within the sidechain and their interaction with the taxol luminal site as well as their effects on signal transmission to other parts of the microtubule structure.[21]

Considering the increased flexibility observed in the solution conformation of *linear*-zampanolide, we wondered if covalent interactions between microtubules and the α,β-unsaturated ketone were affected. Utilizing the previous mass specific conditions reported by Field *et al.* we found that both (-)-zampanolide and (-)-dactylolide modified microtubules to about 25% modification within 30 minutes (see supporting information). However, <4% of total tubulin modification was observed even after 4 hours incubation with *linear*-zampanolide. Thus, while covalent interactions between these marine polyketides and microtubules may play a significant role in their biological activity, rapid functionalization of the tubulin binding site does not correlate with cytotoxicity. As such, it was necessary to confirm that *linear*-zampanolide did induce significant tubulin polymerization under conditions that will not support tubulin polymerization in the absence of a promoting compound. While less than (-)-zampanolide (79%) under identical conditions, *linear*-zampanolide's tubulin polymerization activity (49%) was significantly greater than (-)-dactylolide (2.5%). As final confirmation that *linear*-zampanolide's tubulin polymerization activity correlates to its cytotoxicity, we performed a simple mitotic arrest experiment with PC3 cells, comparing paclitaxel (MI, 54%) and *linear*-zampanolide (MI, 36%).

Conclusion

In summary, we identified a linear zampanolide analog that lacks the constraints of the macrocyclic ring but retains the potent cytotoxic activity of the parent natural product. This effort provides further confirmation that minimization of $A^{1,3}$-strain raised from the C17-methyl and the C15 stereocenter is a key element in controlling its binding confirmation and biological activity. Through computational calculations and NMR studies, we found that the linear analogs display more conformational flexibility than the natural product, as expected, but still populate related and important conformational families. Furthermore, this discovery provides three handles to further diversify the zampanolide scaffold: the C19 acyl group, C9-C11 unsaturated ketone, and the *N*-acyl hemiaminal side chain. This contribution exemplifies the relevance of conformational flexibility in natural products and how structure-conformation-activity relationships can be used to developed new natural product analogues.

Acknowledgements

Financial support by Notre Dame's Chemistry-Biochemistry-Biology Interface Program, an NIH training grant (T32GM075762), and the National Institutes of Health is gratefully acknowledged (GM084922). This work was supported in part by the Intramural Research Program of the Eunice Kennedy Shriver National Institute of Child Health and Human Development, NIH, Bethesda MD, USA. We would like to thank Dr. Evgenii Kovrigin (Director; Magnetic Resonance Research Center, Notre Dame) for assisting with the 2D NMR experiments.

Keywords: zampanolide • conformation • macrocycle • linear • analogue • polyketide

[1] a) R. W. Hoffmann, *Angew. Chem. Int. Ed*. **2000**, *39*, 2054-2070; b) E. M. Larsen, M. R. Wilson, R. E. Taylor, *Nat. Prod. Rep.* **2015**, *32*, 1183-1206.
[2] B. Testa, L. B. Kier, *Med. Res. Rev.* **1991**, *11*, 35-48.
[3] a) R. E. Taylor, Y. Chen, A. Beatty, D. C. Myles, Y. Zhou, *J. Am. Chem. Soc.* **2003**, *125*, 26-27, b) E. M. Larsen, C. Chang, T. Sakata-Kato, J. W. Arico, V. M. Lombardo, D. F. Wirth, R. E. Taylor, *Org. Biomol. Chem.* **2018**, *16*, 5403-5406, c) Z. Zhao, R. E. Taylor, *Org. Lett.* **2012**, *14*, 669-671, d) A. B Smith III, C. A. Risatti, O. Atasoylu, C. S. Bennett, J. Liu, H. Cheng, K. TenDyke, Q. Xu, *J. Am. Chem. Soc.* **2011**, *133*, 14042-14053.
[4] a) J. Tanaka, T. Higa, *Tetrahedron Lett.* **1996**, *37*, 5535-5538, b) Q. H. Chen, D. G. I. Kingston, *Nat. Prod. Rep.* **2014**, *31*, 1202– 1226.
[5] a) J. J. Field, A. J. Singh, A. Kanakkanthara, T. Halafihi, P. T. Northcote, J. H. Miller, *J. Med. Chem.* **2009**, *52*, 7328–7332; b) J. J. Field, B. Pera, E. Calvo, A. Canales, D. Zurwerra, C. Trigili, J. Rodriguez-Salarichs, R. Matesanz, A. Kanakkanthara, S. J. Wakefield, A. J. Singh, J. Jimenez-Barbero, P. Northcote, J. H. Miller, J. A. Lopez, E. Hamel, I. Barasoain, K. H. Altmann, J. F. Diaz, *Chem. Biol.* **2012**, *19*, 686–698.
[6] A. Cutignano, I. Bruno, G. Bifulco, A. Casapullo, C. Debitus and L. Gomez-Paloma, R. Riccio, *Eur. J. Org. Chem.* **2001**, *4*, 775–778.
[7] T. Taufa, A. J. Singh, C. R. Harland, V. Patel, B. Jones, T. Halafihi, J. H. Miller, R. A. Keyzers, P. T. Northcote, *J. Nat. Prod.* **2018**, *81*, 2539–2544.
[8] A. E. Prota, K. Bargsten, D. Zurwerra, J. J. Field, J. F. Diaz, K. H. Altmann, M. O. Steinmetz, *Science* **2013**, *339*, 587–590.
[9] C. J. Radoux, T. S. G. Olsson, W. R. Pitt, C. R. Groom, T. L. Blundell. *J. Med. Chem.* **2016**, *59*, 4314-4325.
[10] E. M. Larsen, M. R. Wilson, J. Zajicek, R. E. Taylor, *Org. Lett.* **2013**, *15*, 5246–5249.
[11] J. L. Henry, M. R. Wilson, M. P. Mulligan, T. R. Quinn, D. L. Sackett, R. E. Taylor, *Med. Chem. Commun*. **2019**, *29*, 800-805.
[12] D. Zurwerra, F. Glaus, L. Betschart, J. Schuster, J. Gertsch, W. Ganci, K. H. Altmann, *Chem. Eur. J*. **2012**, *18*, 16868–16883.
[13] C. P. Bold, C. Claus, B. Pfeiffer, J. Schürmann, R. Lombardi, D. Lucena-Agell, J. F. Díaz, K. H. Altmann, *Org. Lett.* **2021**, *23*, 2238-2242.
[14] J. H. Lii, N. L. Allinger, *J. Am. Chem. Soc*. **1989**, *111*, 8576–8582.
[15] R. E. Taylor, J. Zajicek, *J. Org. Chem*. **1999**, *64*, 7224–7228.
[16] G. Olanders, P. Brandt, C. Sköld, A. Karlén. *Bioorg. Med. Chem.* **2021**, *49*, 116399.
[17] T. M. Brütsch, S. Berardozzi, M. L. Rothe, M. Redondo-Horcajo, J. F. Díaz, K. H. Altmann, *Org. Lett*. **2020**, *22*, 8345−8348.

[18] M. R. Wilson, R. E. Taylor, *Org. Lett.* **2012**, *14*, 3408–3411.
[19] K. Liu, R. E. Taylor, R. Kartika, *Org. Lett.* **2006**, *8*, 5393-5395.
[20] C. P. Bold, M. Gut, J. Schürmann, D. Lucena-Agell, J. Gertsch, J. F. Díaz, K. H. Altmann, *Chem. Eur. J.* **2021**, *27*, 5936–5943.
[21] J. J. Field, B. Pera, J. E. Gallego, E. Calvo, J. Rodríguez-Salarichs, G. Sáez-Calvo, D. Zuwerra, M. Jordi, J. M. Andreu, A. E. Prota, G. Ménchon, J. H. Miller, K. H. Altmann, J. Fernando Díaz *J. Nat. Prod.* **2018**, *81*, 494-505.

Entry for the Table of Contents

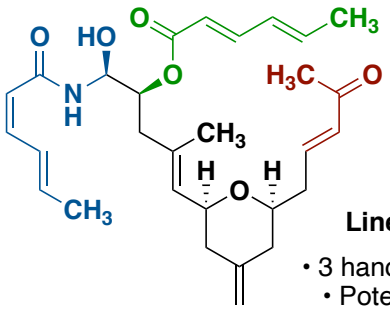

Linear zampanolide

- 3 handles for derivatization
- Potent cytotoxic activity

We developed a linear variant of the potent cytotoxic (–)-zampanolide that retains nanomolar activity towards cancer cell lines. In contrast to medicinal chemistry dogma, these results demonstrate that increased conformational flexibility is not necessarily detrimental to protein binding affinity and biological activity. High-field 2D-NMR, computational modeling, and antiproliferative assays were utilized to develop the conformation-activity relationship profile for this class of marine polyketide. This successful design strategy now provides three new sites for further analog development: *N*-acyl hemiaminal side chain, C19 acyl group, and C9 ketone.

Institute and/or researcher Twitter usernames: @UNDresearch @cumanaga @retaylor61